Best practice in determining key photophysical parameters in triplet–triplet annihilation photon upconversion

Photochemical & Photobiological Sciences
https://doi.org/10.1007/s43630-022-00219-x

PERSPECTIVES

Best practice in determining key photophysical parameters in triplet–triplet annihilation photon upconversion

Fredrik Edhborg[1] · **Axel Olesund**[1] · **Bo Albinsson**[1]

Received: 1 February 2022 / Accepted: 23 March 2022

Abstract
Triplet–triplet annihilation photon upconversion (TTA-UC) is a process in which low-energy light is transformed into light of higher energy. During the last two decades, it has gained increasing attention due to its potential in, e.g., biological applications and solar energy conversion. The highest efficiencies for TTA-UC systems have been achieved in liquid solution, owing to that several of the intermediate steps require close contact between the interacting species, something that is more easily achieved in diffusion-controlled environments. There is a good understanding of the kinetics dictating the performance in liquid TTA-UC systems, but so far, the community lacks cohesiveness in terms of how several important parameters are best determined experimentally. In this perspective, we discuss and present a "best practice" for the determination of several critical parameters in TTA-UC, namely triplet excited state energies, rate constants for triplet–triplet annihilation (k_{TTA}), triplet excited-state lifetimes (τ_T), and excitation threshold intensity (I_{th}). Finally, we introduce a newly developed method by which k_{TTA}, τ_T, and I_{th} may be determined simultaneously using the same set of time-resolved emission measurements. The experiment can be performed with a simple experimental setup, be ran under mild excitation conditions, and entirely circumvents the need for more challenging nanosecond transient absorption measurements, a technique that previously has been required to extract k_{TTA}. Our hope is that the discussions and methodologies presented herein will aid the photon upconversion community in performing more efficient and manageable experiments while maintaining—and sometimes increasing—the accuracy and validity of the extracted parameters.

Keywords Photon upconversion · Triplet–triplet annihilation · Time-resolved emission · Rate constant · Threshold intensity

1 Introduction

Photon upconversion by triplet–triplet annihilation (TTA-UC) is a photophysical process where the energy of two low-energy photons is combined to create one photon of higher energy. The phenomenon of TTA was first described in the 1960s [1] but it was not until 4 decades later that it started to gain more attention because of its potential for increasing the solar energy conversion efficiency of photovoltaics beyond the Shockley–Queisser limit [2, 3]. The research field of photon upconversion has evolved tremendously the past years and the upconversion community has grown to include many research groups around the world. For a description of the progress and the current state of the research field, we refer to recent review articles [4–8].

The process of TTA-UC relies on the interaction of two types of chromophores, called the sensitizer and the annihilator. The sensitizers absorb the incoming photons, and by undergoing intersystem crossing (ISC), they reach the triplet excited state. By a Dexter type interaction with an annihilator in its ground state, the excitation energy is transferred to the annihilator by triplet energy transfer (TET) [9]. Two triplet excited annihilators can then undergo triplet–triplet annihilation (TTA), which is an interaction where one of the annihilators is elevated to an excited state of higher energy and the other returns to the ground state. If the high-energy excited state is of singlet multiplicity, the annihilator can return to the ground state by emitting a photon, i.e., the upconverted fluorescence. In total, two low-energy photons have been absorbed by sensitizers and one photon of

✉ Fredrik Edhborg
edhborg@chalmers.se

✉ Bo Albinsson
balb@chalmers.se

[1] Department of Chemistry and Chemical Engineering, Chalmers University of Technology, 412 96 Gothenburg, Sweden

Published online: 19 April 2022

higher energy has been emitted by an annihilator. By that, the upconversion emission can be regarded as being shifted "anti-Stokes" relative to the excitation light. The overall quantum yield of photon upconversion, Φ_{UC}, is the product of the quantum yields of each sub-step in the process, as written in the following equation:

$$\Phi_{UC} = f\Phi_{isc}\Phi_{TET}\Phi_{TTA}\Phi_{f}. \quad (1)$$

Here, Φ_{isc}, Φ_{TET}, Φ_{TTA}, and Φ_f are the quantum yields of ISC, TET, TTA, and annihilator fluorescence, respectively. f is a spin-statistical factor taking into account the fraction of annihilation events that results in an emissive singlet excited state. Since each TTA event consumes two triplet excited annihilators to produce one singlet excited annihilator (in the case when $f = 1$), the maximum value of Φ_{TTA}, and thereby also of Φ_{UC}, is 0.5 or 50%. The upconversion quantum yield depends on the excitation intensity—it first increases with higher excitation intensity until it reaches a plateau of constant quantum yield. Therefore, it is relevant to define a threshold intensity, I_{th}, that describes the excitation intensity at which Φ_{UC} approaches its high efficiency limit. The upconversion quantum yield, the degree of anti-Stokes shift, and the threshold intensity are parameters that often are used as figures of merit when comparing the performance of upconversion systems. The definition of these parameters and the appropriate way of measuring and reporting them have been discussed in previous articles [10, 11]. These parameters are essential when comparing the performance of the overall upconversion system on material or device level. However, to get insights as to why and how the upconversion system performs the way it does as well as to identify bottlenecks and areas of improvement, other fundamental parameters are essential. In this perspective, we discuss the influence of such parameters as well as the experimental methods to determine them.

The key parameters that are discussed are the triplet energy of the sensitizer and annihilator, the triplet excited state lifetime of the sensitizer and annihilator, the rate constant of TTA (k_{TTA}), I_{th}, and Φ_{TTA}. We discuss various methods to determine these key parameters, including a discussion of how they have been measured traditionally as well as the accuracy of the methods. Based on theory and experimental experience, we propose a new and, relative to other methods, simple method for simultaneous determination of annihilator triplet lifetime (τ_T), k_{TTA}, I_{th}, and Φ_{TTA} from one measurement series of time-resolved upconversion emission, using only standard commercially available equipment and instruments. Our new method is enabled by the nowadays commercially available, easily operated diode lasers, that can be run as a continuous wave (CW) laser as well as time modulated to produce laser pulses with good control over pulse shape, intensity, and frequency. The dual modes of these lasers enable a direct comparison of experiments performed under CW excitation with experiments of time-resolved measurements performed with pulsed excitation. Further, our new method circumvents the need of using more advanced high power ns Q-switched lasers, which traditionally have been used to determine some of the discussed parameters.

This perspective is organized as follows: first comes a general description of how the key parameters of triplet energy, triplet lifetime, and rate constant of TTA influence the performance of the upconversion system. The excitation threshold intensity as a figure of merit for an upconversion system is then discussed. Methods typically applied to determine these parameters are described and evaluated with respect to accuracy, simplicity, and necessary assumptions. Finally, we present the new experimental method for simultaneous determination of annihilator τ_T, k_{TTA}, I_{th}, and Φ_{TTA} from one measurement series of time-resolved upconversion emission.

2 Sensitizer and annihilator triplet energies

Accurate determination of triplet energies is of pivotal importance in TTA-UC since all critical energy exchanges occurs between the triplet states of the interacting compounds.

For efficient triplet energy transfer (TET) to occur, it is beneficial if the annihilator first triplet excited state (T_1) lies lower in energy than that of the sensitizer, thus creating a thermodynamic driving force for this event. Even though endothermic TET has been reported, this often comes at the expense of substantially slower TET rate constants [12, 13]. In addition, a small positive or even negative driving force for TET might enable detrimental back-TET (bTET) from the annihilator to the sensitizer, which will effectively lower the obtainable TET efficiency in the TTA-UC system [14, 15].

The T_1 energy of the sensitizer is also important to consider when analyzing the intersystem crossing (ISC) event following low-energy light absorption. Most heavy-metal containing sensitizers have substantial singlet-to-triplet energy splitting (ΔE_{ST}) of several hundreds of meV, effectively preventing any reverse ISC (rISC) in such molecules. In later years, materials exhibiting thermally activated delayed fluorescence (TADF) have been employed for sensitizing purposes [16–18], in which ΔE_{ST} can take much smaller values down to only tens of meV. The small ΔE_{ST} enables increased anti-Stokes shifts which is beneficial to minimize energy losses during TTA-UC. However, such molecules exhibit pronounced rISC that compete with TET between sensitizer and annihilator, potentially causing the achievable TET efficiency to be lower compared to systems

in which rISC is absent, even if the driving force for TET is substantial. The accurate determination of first excited singlet state (S_1) and T_1 energies of the sensitizer are, thus, needed to properly analyze the TET event, especially when TADF materials are used as sensitizers.

Perhaps even more critical are the singlet and triplet energies of the annihilator compound. Again, it is beneficial to have a thermodynamic driving force for the TTA such that $[2 \times E(T_1) - E(S_1)] > 0$, and efforts have aimed at finding new potential annihilators based on this specific prerequisite [19]. The TTA event may also lead to depopulation through the second triplet excited state (T_2) or the first quintet excited state. The latter is typically too high in energy to be populated, but the former is commonly formed to an appreciable extent in the TTA event since $[2 \times E(T_1) - E(T_2)] > 0$ for most annihilators. The impact of this competing pathway has recently been discussed to some depth, with the main conclusion being that the energy of T_2, and its relation to the energies of S_1 and T_1, is critical to understand the spin-statistical factor, f, which dictates what fraction of annihilator triplets that are ultimately converted into emissive singlets [20]. For f to approach unity the relationship $[2 \times E(T_1) - E(T_2)] < 0$ likely must be fulfilled.

Several different methods are available for measuring the T_1 energy. Many metal-containing sensitizers exhibit room-temperature phosphorescence, and the peak position of this emission band has commonly been used to estimate the T_1 energy, which is suitable for structured phosphorescence emanating from $^3\pi\pi^*$ states. The energies of triplet states with significant charge transfer (CT) character should, however, not be evaluated at the peak of their broad room-temperature emission band, but using the high-energy onset of the emission is believed to yield a more accurate value [21]. One must, thus, consider the triplet state character to make the best estimation of the T_1 energy when using emission emanating from triplet states.

Many sensitizers, and most annihilators, do not exhibit room-temperature emission from their triplet states due to either slow ISC, fast non-radiative decay from the T_1 state, bimolecular quenching, or a combination thereof. To detect the phosphorescence, it is then necessary to incorporate the compound of interest in a material which upon cooling to, e.g., 77 K forms a glassy matrix. This effectively turns off the bimolecular non-radiative relaxation pathways from the triplet state and, in many cases, allows for phosphorescence to be detected even in materials where ISC is slow. Alternatively, one can in some cases use direct singlet-to-triplet (S–T) absorption to populate the triplet and subsequently observe the phosphorescence [22]. Heavy atom solvent additives, such as ethyl iodide, can be added to enhance spin–orbit coupling, which in turn further promotes ISC/S–T absorption, facilitating the detection of still relatively weak emission signals [23, 24].

Great care must be taken during experiments to ensure that the detected emission is in fact phosphorescence from the compound of interest. With respect to this, the direct S–T absorption method has a few advantages. First, the direct population of the triplet state results in emission only from the triplet, meaning that steady-state spectra may in some cases be collected without using any time-gated detection. If normal singlet-to-singlet (S–S) absorption plus ISC is instead used, one must have a sufficiently long gating time to exclude any short-lived fluorescence from being collected by the detector. Second, S–T absorption takes place at longer wavelength than S–S absorption, and it can often be expected that any impurities in the sample absorbs less of a longer wavelength excitation light. However, if in doubt one should validate the origin of the emission signal, e.g., by the use of excitation spectra.

Examples of phosphorescence spectra measured by each of the above discussed methods are presented in Fig. 1 for zinc octaethylporphyrin (ZnOEP) dissolved in 2-methyltetrahydrofuran (MeTHF) as a model compound. Figure 1a shows the room-temperature steady-state absorption spectrum as well as a gated emission spectrum at 85 K. ZnOEP is slightly fluorescent at room temperature, but once the sample is cooled to 85 K, where the solvent has formed a solid glass, also phosphorescence can be extracted from ZnOEP in a gated emission spectrum. For collecting a gated emission spectrum, a pulsed excitation light source is used and the emission from the sample is collected for a certain detection time with a time delay after the end of the excitation pulse. By that, the long-lived emission of phosphorescence can be isolated from the short-lived fluorescence and other background signals, such as scattering and stray light from the excitation source. By choosing a short (or negative) delay time, both the fluorescence and phosphorescence signal can be obtained in the same spectrum, as seen in Fig. 1a. With a longer delay time, the fluorescence can totally be excluded so that only the long-lived phosphorescence is obtained in the emission spectrum, as seen in Fig. 1b. The same spectral profile of the phosphorescence spectrum was also obtained with S-T excitation at 660 nm (Fig. 1c), even though the phosphorescence intensity was much lower. Phosphorescence decay upon excitation at 405 and 660 nm (Fig. 1d, e) show that the same phosphorescence lifetime is obtained independent of excitation wavelength, confirming that the emission spectrum obtained with S–T excitation origins from the same species as with S–S excitation. The black line in Fig. 1c shows a steady-state emission spectrum upon 660 nm excitation. The signal in this spectrum originates partly from the weak ZnOEP phosphorescence but is overlayed with scattering, straylight, and emission from minor impurities. A comparison of this spectrum with the gated emission spectrum in the same graph shows the power of using time

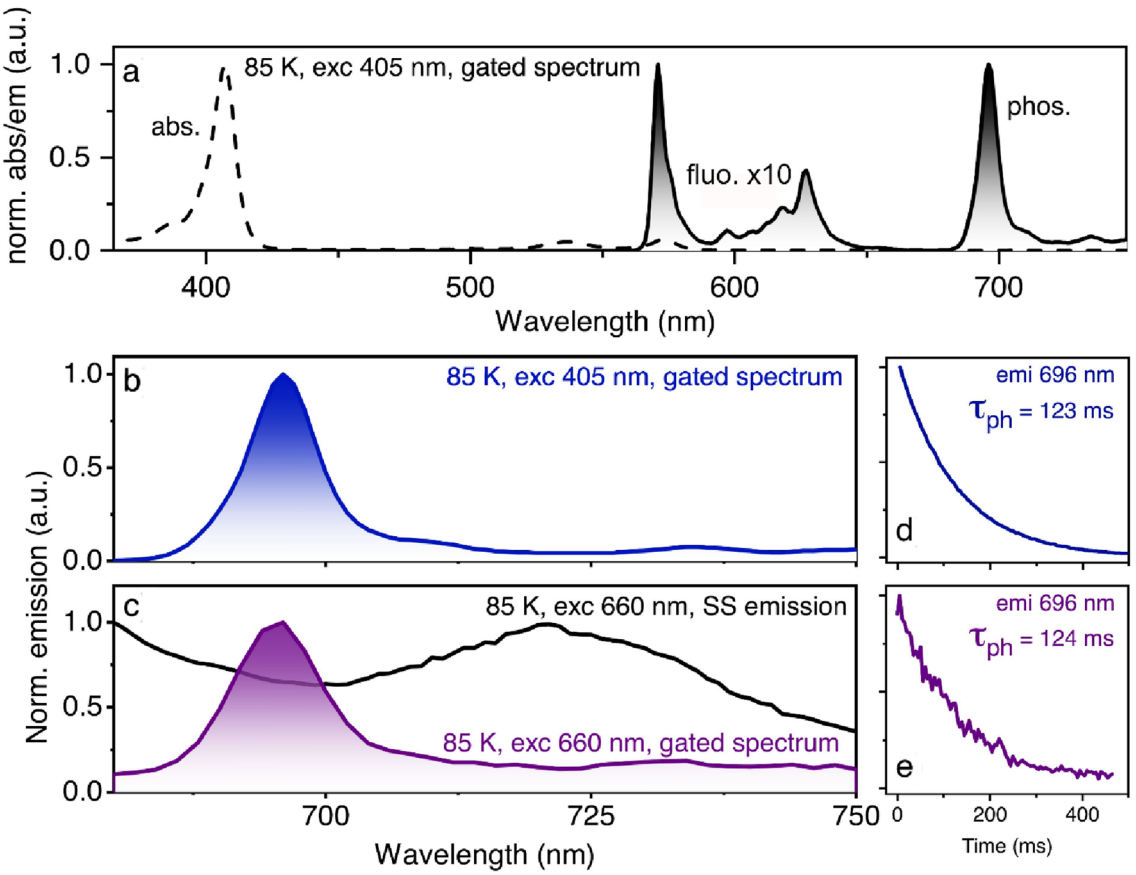

Fig. 1 Normalized absorption and emission spectra of ZnOEP in MeTHF. **a** Steady-state room-temperature absorption spectrum together with 85 K gated emission spectrum showing both fluorescence and phosphorescence (gating parameters: population time 21 ms, delay time − 1 ms, detection time 20 ms). **b**, **c** Gated emission spectrum at 85 K, excited using a modulated CW laser with S–S excitation at 405 nm (population time 20 ms, delay time 0 ms, detection time 20 ms) and S–T excitation at 660 nm (population time 20 ms, delay time 5 ms, detection time 30 ms), respectively. Black line in **c** shows a corresponding steady-state emission spectrum recorded using 660 nm CW laser excitation. **d**, **e** Phosphorescence decay with S–S and S–T excitation, respectively

gating to filter out small signals of long-lived emission components that otherwise are hidden in the steady-state background signal.

Using phosphorescence measurements at low temperature will only give an estimate of the true T_1 energy at room temperature. One must consider, e.g., rotational flexibility of the molecule as it is known that low-temperature phosphorescence of rotationally flexible molecules typically underestimates the room-temperature T_1 energy [25]. Instead of using phosphorescence measurements, one can employ triplet sensitization protocols to determine the T_1 energy of a compound. While phosphorescence measurements are somewhat more feasible, the triplet sensitization approach allows for determination of T_1 at room-temperature and likely yields a value that is more relevant for applications involving room-temperature TET in solution.

Assuming dynamic quenching that follows Stern–Volmer kinetics, the Sandros equation (Eq. 2) can be used to determine the T_1 energy of a compound [26]:

$$k_{\mathrm{TET}} = \frac{k_{\mathrm{diff}}}{1 + \exp\left(-(E_{\mathrm{T,D}} - E_{\mathrm{T,A}})/k_{\mathrm{B}}T\right)}. \quad (2)$$

Here, k_{TET} is the rate constant for TET ($\mathrm{M}^{-1}\ \mathrm{s}^{-1}$), k_{diff} is the rate constant of TET at the diffusion limit, $E_{\mathrm{T,D}}$ and $E_{\mathrm{T,A}}$ are the donor and acceptor T_1 energies, respectively, k_{B} is the Boltzmann constant, and T is temperature. To obtain the T_1 energy, a series of measurements is performed in which the compound of interest interacts with a chosen number of different molecules with known T_1 energies. One can use the compound of interest either as the donor or the acceptor. If the compound shows phosphorescence it is best used as a donor since then any type of triplet quencher with known T_1 energies (emissive

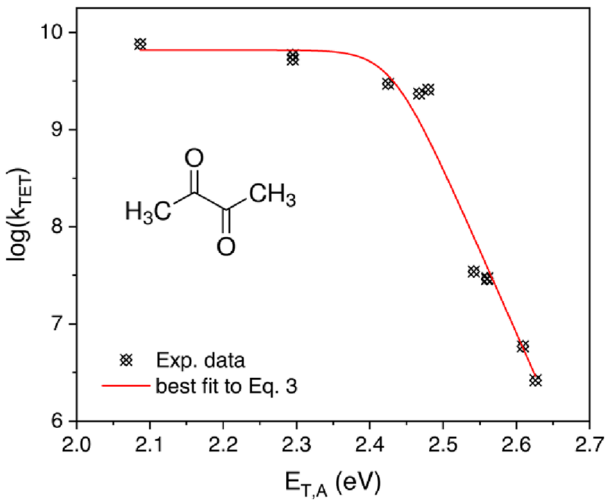

Fig. 2 Sandros plot obtained from phosphorescence quenching of biacetyl (inset) with a series of triplet acceptors in benzene. Data points adapted from ref [26]

or not) can be employed. If the investigated compound, which may or may not show phosphorescence, is used as an acceptor, then the used series of donors need to be emissive if one wants to avoid using transient absorption to determine k_{TET} for the different donor/acceptor pairs.

Following the determination of k_{TET} for all donor/acceptor pairs these may be visualized and analyzed in a Sandros plot. An example of a Sandros plot is shown in Fig. 2 where the rate constant of TET from biacetyl to a series of triplet acceptors is analyzed. The data are here plotted with the T_1 energy of the acceptors on the abscissa and the logarithm of k_{TET} on the ordinate, and the data are then fitted to the following equation:

$$\log(k_{TET}) = \log\left(\frac{k_{diff}}{1+\exp\left(-(E_{T,D}-E_{T,A})/k_BT\right)}\right). \quad (3)$$

Figure 2 shows the data from Sandros' seminal 1964 paper where the triplet state of biacetyl was investigated using phosphorescence quenching [26]. The data have been fitted to Eq. 3, yielding a T_1 energy of 2.43 eV, which is very close to that obtained from room-temperature phosphorescence in benzene [27]. Interestingly, the value obtained from the quenching experiments is slightly higher than that obtained using the room-temperature phosphorescence peak, but significantly lower than if the onset of phosphorescence is used, thus highlighting how different methodologies indeed yield quite different results (see ref. [27] for the room-temperature phosphorescence spectrum of biacetyl). Situations where more elaborate kinetics than those developed by Sandros must be used may arise, which has been exemplified in later works [28, 29].

3 Sensitizer and annihilator triplet lifetime

As mentioned earlier, many sensitizers exhibit room-temperature phosphorescence or TADF. These processes both involve the T_1 state and measurements of time-resolved emission decay of such signals may be used to measure the triplet lifetime, τ_T, of many sensitizer compounds. Alternatively, nanosecond transient absorption (nsTA) may be used, in which the time-resolved decay of triplet–triplet absorption signals are probed.

When determining τ_T of sensitizers one should not use too high concentrations or excitation intensities. Many sensitizers may undergo TTA themselves, resulting in increased non-radiative decay. This leads to an observed (apparent) lifetime shorter than the real intrinsic lifetime. Such effects may be hard, or impossible, to avoid in nsTA due to the need for high excitation intensity and high concentration. For this reason, we recommend that time-resolved emission should preferentially be used to determine τ_T when possible. For time-resolved emission, a concentration of some few μM is typically enough for decently emitting compounds. Sensitizer TTA might be hard to avoid entirely during such measurements as well, but the second-order channel can be

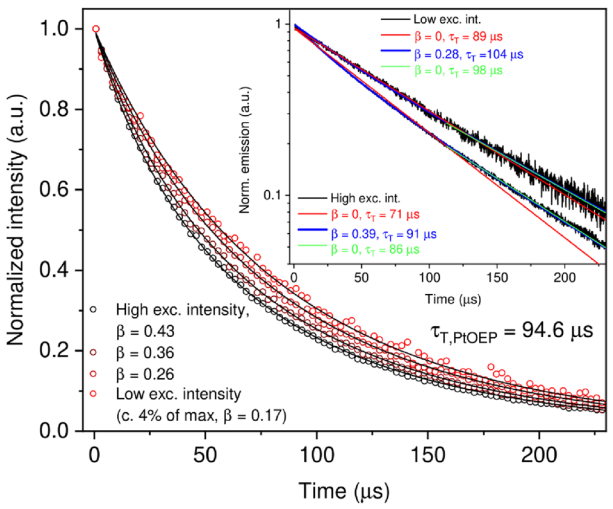

Fig. 3 Phosphorescence (λ_{em} = 650 nm) decay of 10 μM PtOEP in deaerated toluene at different intensities of ns pulsed excitation (λ_{exc} = 532 nm, < 10 ns pulse length), excitation intensity 0.03–0.6 mJ/pulse. Solid lines are global fits to Eq. 4 with τ_T as a shared global fitting parameter and β as a free fitting parameter, n = 1. Inset: PtOEP emission decay at high and low excitation intensities with best fit to Eq. 4 with β as a free fitting parameter (blue lines) or with β fixed to zero (red/green lines), n = 1. Only the later parts of the decays are used to obtain the green line fits, yielding lifetimes more similar to that of the global fitting procedure

accounted for during the fitting procedure. One example of this is shown in Fig. 3 where the phosphorescence lifetime of platinum octaethylporphyrin (PtOEP) is investigated with respect to excitation intensity (I_{EX}), using a ns Q-swiched laser as excitation source. As can be seen, the decay kinetics of PtOEP phosphorescence is slightly shortened at higher I_{EX}, owing to TTA between PtOEP triplets. To extract τ_T while taking the effect of TTA into account, the emission decay traces recorded at various excitation intensities are analyzed using the following equation (the derivation of this equation is described in Sect. 6):

$$I(t) \propto \left[{}^3E^*(t)\right]^n = \left(\left[{}^3E^*\right]_0 \frac{1-\beta}{\exp\left(\frac{t}{\tau_T}\right) - \beta} \right)^n . \quad (4)$$

Here, $I(t)$ is the time evolution of the measured emission signal, $\left[{}^3E^*(t)\right]$ is the triplet concentration of the emitting species at time t, $\left[{}^3E^*\right]_0$ is the triplet concentration at time zero, τ_T is the triplet lifetime, and β is a dimensionless parameter indicating what fraction of triplets that initially decay by second-order channels. n is a parameter describing how the emission intensity depends on the concentration of molecules in the triplet excited state. For phosphorescence, the emission intensity is directly proportional to the concentration and $n=1$. If the studied emission is upconversion resulting as a subsequent event following TTA between two triplet excited annihilators, the emission intensity is proportional to the square of the triplet excited annihilator concentration, i.e., $n=2$. By fitting the emission decays in Fig. 3 in a global fit, i.e., all decays share the same global τ_T, the PtOEP triplet excited state lifetime was determined to $\tau_T = 95$ µs. Here, each decay is fitted to individual values of β, since the influence of TTA on the decay kinetics will vary with I_{EX}. β may take values between 0 and 1, with 0 indicating no initial TTA (Eq. 4 then takes the form of a single exponential decay) and 1 indicating that all triplets initially decay by TTA.

As seen from the inset of Fig. 3, the global fitting procedure results in a different τ_T than if Eq. 4 (with $n=1$) is used for single traces only: the high and low-intensity excitation decays result in shorter and longer τ_T, respectively. The comparison highlights that different experimental settings can yield different results if the global fitting procedure is not employed. Best fits to single exponentials ($\beta=0$) are included for comparison as well, which become increasingly inaccurate at higher I_{EX}, yielding shorter τ_T. An alternative fitting procedure is to do a tail fit using only the later parts of the decay when most of the bimolecular events have occurred. Such a fit is included in the inset in Fig. 3 and gives a slightly shorter or longer lifetime than the global fit, depending on the excitation intensity used during the measurement. Since bimolecular decay processes never can be totally excluded, the triplet lifetime obtained from a tail fit should be regarded as a low-end estimate of the actual lifetime in cases where only one excitation intensity is used.

Even more important for TTA-UC is arguably τ_T of the annihilator, a parameter commonly determined from time-resolved emission of upconverted light. The fitting procedures to determine τ_T, however, vary significantly, but typically Eq. 4 is the starting point. Since two triplet annihilators must interact to form emissive singlets, $n=2$ must be used. Many times, only the tail of the measured decay (where the influence from TTA on the kinetics is smaller) is used during the fitting procedure, and Eq. 4 with $\beta=0$ is then used [30, 31]. The measured time constant (often referred to as τ_{UC}) will then equal $\tau_T/2$. Alternatively, a similar procedure to that we propose for the determination of τ_T of the sensitizer has been used, in which τ_T is determined by globally fitting UC emission decays acquired at varying excitation intensities [15, 32].

In the example shown in Fig. 4, PtOEP and 9,10-diphenylanthracene (DPA) are used as the sensitizer and annihilator, respectively. The sample was excited using a modulated CW diode laser giving a square-shaped excitation pulse, see Sect. 6 for further description. The decays of upconverted emission recorded at various excitation intensities are globally fitted to Eq. 4 with $n=2$ with a shared global τ_T, yielding a triplet lifetime of 8.0 ms. This value stand in contrast to that achieved by other means of fitting, as can be seen from Fig. 4b. The exponential tail fits consistently yield shorter τ_T than that of the global fit, with τ_T almost cut in half at higher excitation intensity. Using a single decay and fit this to Eq. 4 with $n=2$ also yields slightly different values from that obtained by the global fitting, as was also the case in Fig. 3. As can be seen, the global fitting procedure yields a τ_T value (8.0 ms) in between those from the single trace fits (7.6 and 8.9 ms, respectively) measured at high and low excitation intensity, which is to be expected.

To summarize, the influence from TTA on emission emanating from reactions on the triplet surface can, in most cases, not be disregarded during transient analysis. We urge the field to, when applicable, move away from the simple but incorrect way of using exponential tail fits to a single decay to determine the triplet lifetime of sensitizer and, more importantly, annihilator species. Instead, we propose that several decays at varying excitation intensities should be collected, which is followed by a global fitting procedure in which the influence of the TTA event is accounted for. We note that the annihilator τ_T in certain (quasi) solid-state systems, such as those based on polymer nanodroplets, has been reported to not show any dependence on excitation intensity due to nano-confinement [33]. Either way, performing

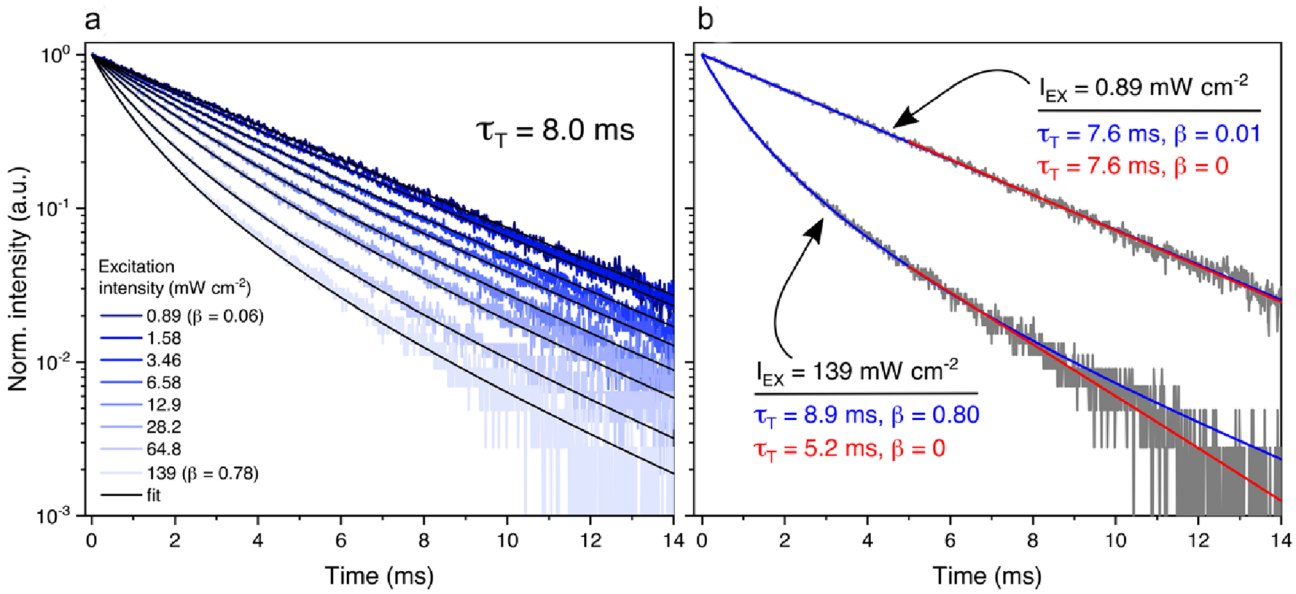

Fig. 4 **a** Upconverted emission decay of a DPA/PtOEP sample in deaerated toluene at different intensities of pulsed 532 nm excitation (modulated CW laser excitation, 35 ms population time). Solid lines are global fits to Eq. 4 with $n=2$ and a shared τ_T. **b** Upconverted emission decay of a DPA/PtOEP at the highest and lowest excitation intensities, respectively, with best fit to Eq. 4 with τ_T and β as fitting parameters (blue lines) or tail fitted to Eq. 4 with τ_T as fitting parameter and β fixed to zero (red lines), $n=2$

excitation intensity dependent measurements will yield valuable information about the system at hand.

Different methodologies are causing reported τ_T to vary a lot, and as an example you can find reports for DPA from around 1 to almost 10 ms in liquid solution [32, 34–36]. Another reason for these discrepancies is that it is inevitable that the O_2 concentration will vary between samples from different studies. O_2 is an excellent quencher of triplet states and to afford TTA-UC, as much O_2 as possible should be removed (at least for liquid samples). Several different methods for degassing samples exist, and although no method can remove all O_2 from a sample, we argue that (liquid) samples for TTA-UC should be prepared either by freeze–pump–thaw or in a glovebox. Simply bubbling with N_2 or argon is—in our experience—insufficient to properly degas the sample, and the reproducibility of such procedures is much lower compared to freeze-pumping or glovebox preparation.

The observed τ_T of the annihilator might also be affected by back-TET (bTET) from annihilator to sensitizer and is of significance especially when high sensitizer concentrations are used. As an example, τ_T of DPA has been determined to be only 140 µs when [PtOEP] = 1 mM, which is explained in full by the presence of 1 mM PtOEP [15]. This effect can, however, be disregarded if the sensitizer concentration is low enough or if the energy gap between the triplet states of sensitizer and annihilator is large enough, further emphasizing the need for the proper determination of these values.

We also want to highlight that systems using transmitter-bound nanocrystal sensitizers (NCs) based on, e.g., perovskites or chalcogenides, typically exhibit much shorter annihilator τ_T than those using molecular sensitizers. For instance, τ_T of DPA has been measured to 150 µs using gold-doped CdSe NCs [37] and τ_T of the UV-emitting species 2,5-diphenyloxazole (PPO) has been measured to around 50 µs [38] using CdS NCs as sensitizers, as compared to 1.3 ms when using an organic sensitizer [13]. The reason for this discrepancy is unclear but is potentially related to observations of thermally activated bTET from the bound transmitter to the NCs [39]. Nonetheless, the shorter τ_T most likely contributes to the lower TTA-UC efficiencies typically found in NC-based systems.

4 The triplet–triplet annihilation rate constant, k_{TTA}

Following TET from sensitizer to annihilator, the upconverted emission is created by means of TTA between two triplet excited annihilators. Similar to TET, this is a diffusion-controlled process in liquid samples, but the kinetics of the TTA event has gained relatively scant attention so far despite its obvious importance for TTA-UC systems. The determination of k_{TTA} has typically been achieved by means of nanosecond transient absorption (nsTA) measurements, in which the kinetics of annihilator triplet absorption have been monitored to extract this rate constant [40–43].

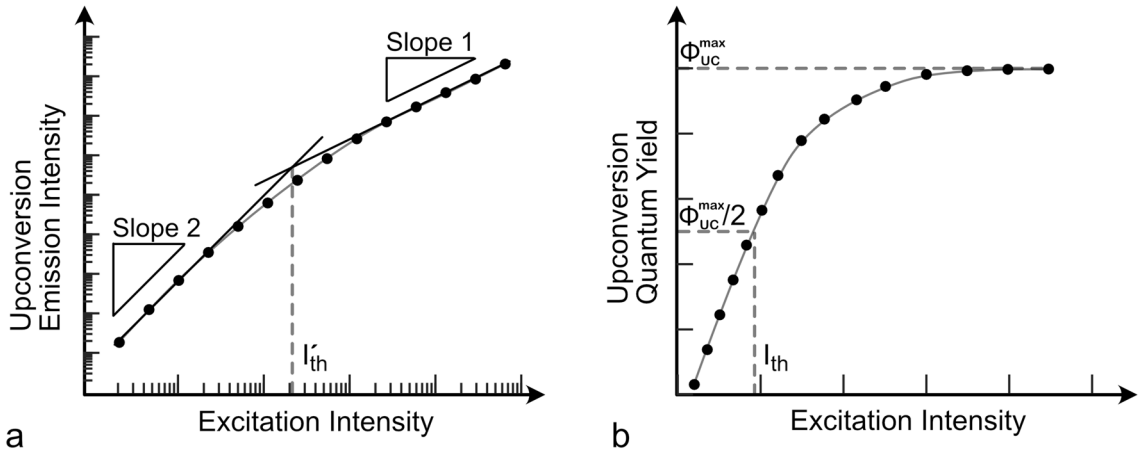

Fig. 5 Schematic illustration of the excitation intensity dependence of upconversion emission intensity (**a**) and upconversion quantum yield (**b**). The threshold intensity is identified in accordance with the traditional method in (**a**) and by the formal definition in (**b**). Note that the threshold intensity identified in (**a**) corresponds to half the value of the threshold intensity defined in (**b**), as discussed in the text

In a few studies, the emission of upconverting samples has been probed in addition to the triplet absorption to extract k_{TTA} [32, 36]. Using nsTA for determining k_{TTA} requires the accurate determination of molar extinction coefficients of the annihilator triplet excited states in addition to the possibility to perform accurate measurements of weak triplet absorption signals. It is typically performed using a short (ns) and intense laser excitation pulse, which can be difficult to control and give rise to, e.g., significant sensitizer-sensitizer annihilation. In addition, the high optical density that typically is required at the excitation wavelength in order to yield a proper TA signal potentially leads to inhomogeneous excitation and thereby inhomogeneous TTA kinetics within the sample volume that is probed.

Our group has recently reported a method in which k_{TTA} can be extracted using only measurements of time-resolved emission [13]. We will return to the full description of this method in Sect. 6, but instead of using a short (< 10 ns), high-energy laser pulse, we used a commercially available CW diode laser in modulated mode, allowing for much lower excitation intensities and excellent temporal control of the pulse. This recent report studied UV-emitting annihilators for which no k_{TTA} values (except PPO [40]) had been reported so far. Interestingly, the value previously obtained for PPO using nsTA (5×10^9 M^{-1} s^{-1}) is approximately three times higher than that obtained using our new method. As will be shown below, the same trend appears for DPA: the k_{TTA} values obtained using nsTA (ca 2.5×10^9 M^{-1} s^{-1}) are about three times higher than those extracted herein (vide infra).

5 The threshold intensity, I_{th}

Because of the bimolecular nature of TTA, the rate of TTA depends quadratically on the concentration of triplet excited annihilators, and thereby also on the excitation intensity. At low excitation intensities, the probability of two triplet excited annihilators encountering each other and undergo TTA within its excited state lifetime is low, but it increases quadratically with excitation intensity. At high enough excitation intensity, the concentration of triplet excited annihilators can be so high that most annihilator triplets find an annihilation partner within their excited state lifetime, which makes the probability of triplet depopulation by TTA approach unity. This behavior gives rise to a complex excitation intensity dependence of the upconversion emission intensity, which increases quadratically at low excitation intensities but switch to a linear increase at high excitation intensities [44]. This can be seen as a shift from slope 2 to slope 1 in a double logarithmic plot, as illustrated in Fig. 5a. This behavior is also reflected in the quantum yield of upconversion, which increases at low excitation intensities but converges to a plateau of constant quantum yield at high excitation intensities, as seen in Fig. 5b. A parameter that often is used to characterize an upconversion system is the threshold intensity, I_{th}. I_{th} is defined as the steady-state excitation intensity at which half of the annihilator triplet population depopulates by TTA. An equivalent definition is the excitation intensity at which the upconversion quantum yield reaches half of its maximum value [45]. It should be noted that the threshold intensity is not a parameter of the upconversion chromophores but should rather be seen as a figure of merit of the upconversion sample as a whole because the threshold intensity depends on the concentration of both sensitizer and annihilator, the oxygen content (which

affects the triplet excited state lifetimes), and viscosity etc. Therefore, when reporting I_{th}, care should be taken to always report the composition of the upconversion sample and the experimental conditions under which it was measured.

The most common way to determine the threshold intensity is by measuring the upconversion emission intensity at various excitation intensities, plot the data in a graph with logarithmic scales, and find the intersect between the straight lines fitted to slope 2 and 1 in the low and high excitation regimes, respectively, as illustrated in Fig. 5a. However, in a recent publication by Murakami et al. it has been shown that the threshold intensity achieved using this method, I_{th}', does not represent the threshold intensity by the formal definition, I_{th} [44]. In fact, it is in this publication concluded that the excitation intensity where the lines of slopes 2 and 1 intersect corresponds to half the value of I_{th}, a conclusion that has been verified by us. That the upconversion emission intensity asymptotically approaches slope 2 and 1 in the double logarithmic excitation intensity plot is based on theoretical arguments and holds for both pulsed and CW excitation [45–47]. However, its derivation is based on a couple of assumptions that not necessarily always are valid. For example, slope l is not necessarily achievable if the annihilator concentration or the annihilator triplet lifetime is too low/short. Further, other competing processes can become prominent at high excitation intensities or high sensitizer concentration, such as sensitizer-sensitizer self-annihilation, which competes with sensitizer-to-annihilator TET and reduces the effective upconversion quantum yield [15, 48, 49]. It has also been shown that some specific upconversion materials have other excitation intensity dependencies due to effects of nano-confinement and inhomogeneous size of the upconversion sites, for which an alternative expression for the excitation intensity dependence can be derived mathematically [33, 50]. There are several examples in the literature where the reported value of I_{th} is obtained by fitting the upconversion emission intensity at low and high excitation intensities to lines with slope approximately 2 and approximately 1 in the double logarithmic plot. This may yield a better fit to the experimental data but is not correct from a theoretical view on how I_{th} is defined. For cases in which the upconversion emission intensity for any reason does not reach a fully quadratic and linear behavior in the low and high excitation intensity regimes, we instead suggest using our new method to determine the threshold intensity, described in the next section. We argue that this new method is more correct from a theoretical perspective and more accurate in an experimental perspective compared to the traditional methods for measuring threshold intensity. This is because it is not based on the assumption that the upconversion emission follows the idealized behavior with a quadratic and linear region, as discussed as follows.

6 New method for simultaneous determination of k_{TTA}, τ_T, I_{th}, and Φ_{TTA}

Based on the discussions above and in light of the nowadays commercially available easily operated diode lasers, we propose a new method for experimentally determining k_{TTA}, τ_T, I_{th}, and Φ_{TTA} from only one series of time-resolved upconversion emission measurements. The method has already been used in our group and is briefly described in a recent publication [13]. We will here give a more detailed description of the method, the assumptions it is based upon, and compare it to previously used procedures with respect to accuracy and simplicity.

Our new method is an extension to the protocol for determining τ_T of an annihilator by globally fitting upconversion emission decay traces measured at various excitation intensities, as described in Sect. 3. The experimental setup of the new method is shown schematically in Fig. 6a and the data acquisition procedure is illustrated in Fig. 6b, c. Instead of using a ns pulsed laser, a modulated CW diode laser is used to excite the sample with a square-shaped pulse. The time of the laser-on/off cycles is controlled using a pulse generator that triggers the laser. The emission from the sample is passed through a short-pass filter or a monochromator so that only the upconversion emission reaches the detector, from which the emission signal is read by an oscilloscope. For each pulse cycle, the sample is excited with constant intensity during the laser-on time and the subsequent decay of the upconversion emission signal during the laser-off time is recorded. With this experimental setup, UC emission decay traces can be achieved where the excitation pulse is controlled with high precision in both duration time and intensity. Further, one and the same laser can be used as excitation source for both time-resolved and steady-state experiments, a feature that will be important later to extract I_{th} and Φ_{TTA}.

The key instrument in this experimental setup is the modulated CW laser that must be able to be modulated fast enough for the experiment. Modern diode laser can often be modulated with frequencies up to several kHz or MHz, which is orders of magnitude higher frequencies than what is needed for this type of experiment. The most important parameter for our experiment is the fall time of the laser, i.e., how fast the excitation intensity can switch off from full power when turning from laser-on to laser-off cycle. This (together with the detector and the oscilloscope) sets the response time of the experimental setup. For the laser used in our setup, the fall time is specified in the data sheet to < 2 µs and other laser models in the same family have both rise times and fall times specified to some few tens of ns. By this, this class of lasers exceeds the requirements for probing upconversion emission signals on the time scale of 10 µs–10 ms.

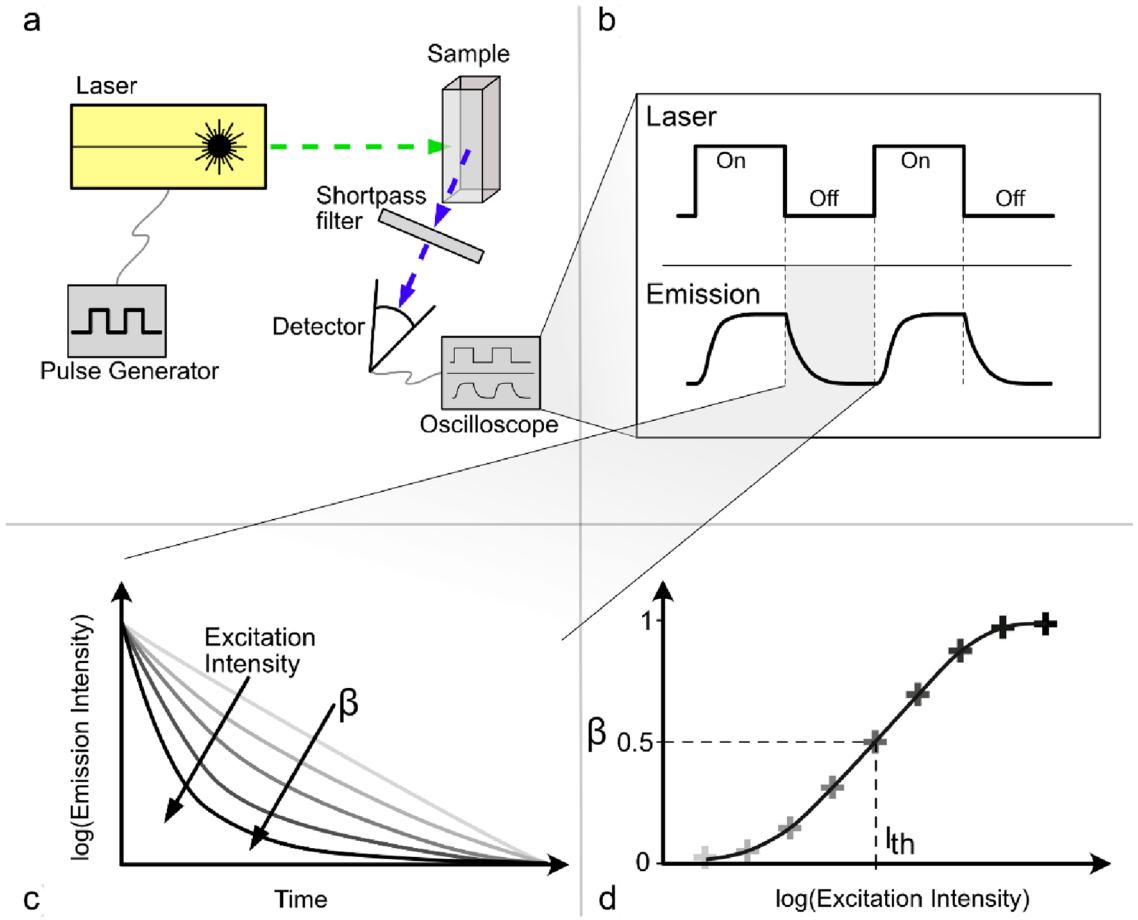

Fig. 6 The principles of our new method for determining k_{TTA}, k_T, and I_{th}. **a** Schematic outline of the experimental setup. **b** The time evolution of the upconversion emission signal relative to the phase of the modulated CW laser. **c** Decay traces of the upconversion emission during the laser-off cycle in a semilogarithmic plot at various excitation intensities. **d** Identification of I_{th} in a semilogarithmic graph of β obtained from a global fit of upconversion decay traces, plotted against excitation intensity

To describe the fitting procedure from which k_{TTA} will be extracted, we start from the beginning with the rate equations that eventually lead to an expression for the time-resolved upconversion emission. Values of τ_T, Φ_{TTA}, and I_{th} will fall out as byproducts from the fitting procedure, as described as follows. The concentration of triplet excited annihilators within the excitation volume of the upconversion sample, $[^3A^*]$, at time, t, is given by the rate equation in the following equation:

$$\frac{\mathrm{d}[^3A^*]}{\mathrm{d}t} = k_{gen} - k_T[^3A^*] - 2k_{TTA}[^3A^*]^2. \quad (5)$$

Here, k_{gen} is the rate of generation of triplet excited annihilators by triplet sensitization from the sensitizer. The term $k_T[^3A^*]$ is the rate of depopulation of triplet excited annihilators by spontaneous decay to the ground state, including all (pseudo) first-order kinetics decay mechanisms ($k_T = 1/\tau_T$). The term $2k_{TTA}[^3A^*]^2$ is the rate of depopulation by TTA. This equation can be written in a number of ways and is here written with the unit mol·dm^{-3}·s^{-1}. The rate constants k_T and k_{TTA}, thus, have the units s^{-1} and s^{-1}·M^{-1}, respectively. The factor 2 in front of k_{TTA} is here explicitly written out to take into account that two annihilator triplets are annihilated in each annihilation event. Equation 5 is a simplified version of the system of rate equations necessary to accurately describe the time evolution of the triplet excited annihilator. The full system of rate equations can be found in the Supporting Information and the assumptions made to derive Eq. 5 are discussed as follows. When the laser turns off after an excitation cycle, k_{gen} becomes zero and the annihilator triplet population starts to decay. The decay profile of the annihilator triplet concentration is given by the analytical solution to the decaying part of Eq. 5 [46, 51]:

$$[^3A^*](t) = [^3A^*]_0 \frac{1-\beta}{\exp\left(\frac{t}{\tau_T}\right) - \beta}. \quad (6)$$

Here, $\tau_T = 1/k_T$ is the triplet lifetime of the annihilator. $\left[{}^3A^*\right]_0$ is the concentration of triplet excited annihilators at time zero, that is, at the moment when the laser is turned off. Note that Eq. 6 describes the time profile of the triplet excited annihilator concentration. The upconversion emission intensity, which is the quantity that is observed experimentally, is described by Eq. 4 (with $n = 2$) [46, 52]. As described in Sect. 3, k_T and β can be obtained by globally fitting upconversion emission decay traces recorded at various excitation intensities to Eq. 4. β, which was not considered explicitly in Sect. 3, is defined in the following equation:

$$\beta = \frac{2k_{TTA}\left[{}^3A^*\right]_0}{k_T + 2k_{TTA}\left[{}^3A^*\right]_0}. \tag{7}$$

From Eq. 7 it can be seen that if $\left[{}^3A^*\right]_0$ was known, then also k_{TTA} could be extracted from the global fit of upconversion emission decay traces. If a ns pulsed laser was used as excitation source in an upconversion emission experiment, it would be difficult to estimate $\left[{}^3A^*\right]_0$ because of the very short and intense excitation pulse. In comparison, if a CW laser is used as excitation source, the population of triplet excited annihilators will after some few milliseconds of excitation reach a steady-state concentration where the generation rate of annihilator triplets equals the rate of depopulation. Excitation using a square-pulse modulated CW laser can be regarded as an intermediate between pulsed and CW excitation; it enables measurements of emission decay kinetics after an excitation pulse with the very important feature that the sample can be in a well-defined state at time zero of the decay. By making the laser-on cycle long enough, the population of excited species will have reached the steady-state concentration when the laser-off cycle starts and the emission decay is recorded. In that case, $\left[{}^3A^*\right]_0$ can be identified as the steady-state concentration at the given excitation intensity and be calculated from Eq. 5 by setting $\mathrm{d}\left[{}^3A^*\right]/\mathrm{d}t = 0$:

$$0 = k_{exc}\Phi_{isc}\Phi_{TET} - k_T\left[{}^3A^*\right]_0 - 2k_{TTA}\left[{}^3A^*\right]_0^2. \tag{8}$$

Here, the rate of annihilator triplet generation has been defined as $k_{exc}\Phi_{isc}\Phi_{TET}$, where k_{exc} is the rate of excitation of sensitizers (that is, mole of photons absorbed by sensitizers per time and volume) and Φ_{isc} and Φ_{TET} are the quantum yields of ISC of the sensitizer and TET from sensitizer to annihilator, respectively. k_{exc} can be calculated from the ground state absorbance of the sample at the excitation wavelength together with the laser cross section area and laser power during the laser-on time. Φ_{TET} can typically be obtained from a separate phosphorescence quenching experiment. By this, Eqs. 7 and 8 constitutes a solvable equation system where k_{TTA} and $\left[{}^3A^*\right]_0$ are the only unknown parameters. Thus, k_{TTA} and k_T can be obtained as the global fitting parameters when a series of upconversion emission decay traces, obtained at various excitation intensities, are fitted to Eq. 4 (with $n = 2$) in combination with Eqs. 7 and 8.

As stated in the introduction to this section, I_{th} can also be extracted from the experiment described above. The derivation of this requires a closer look at the parameter β. Comparing the numerator and denominator of Eq. 7 with the two right hand terms in Eq. 5 it can be seen that β describes the initial relative rate of triplet decay by TTA in relation to the total initial rate of triplet decay [51, 52]. Since I_{th} is defined as the steady-state excitation intensity at which half of the annihilator triplet population decays by TTA (see Sect. 5), it can be concluded that I_{th} must be equal to the excitation intensity at which $\beta = 0.5$, provided that the sample has reached the steady-state concentration during the laser-on excitation cycle. Hence, I_{th} can easily be obtained from a plot of the fitted value of β as a function of excitation intensity, as illustrated in Fig. 6d.

Another interesting property of β is its relation to the quantum yield of TTA, Φ_{TTA} [37, 53]. In the steady-state approximation, the quantum yield of a process equals the rate of the process divided by the rate of all other competing processes. Since β here is calculated from the upconversion emission decay from a sample initially in steady state, it can with the same argument as above be concluded that Φ_{TTA} and β are related by the following equation:

$$\Phi_{TTA} = \beta/2. \tag{9}$$

The factor $^1/_2$ is here included to account for the theoretical maximum quantum yield of TTA being 0.5. With a known value of Φ_{TTA} it is possible to calculate the spin-statistical factor, f, from the observed upconversion emission quantum yield using Eq. 1. In the literature, it is common that f is calculated with a Φ_{TTA} that is assumed to be 0.5 in the high excitation intensity regime. With our new method, f can be determined using purely experimentally determined quantum yields without the need for such assumptions [13]. This is possible because the same laser that is used modulated for the time-resolved experiments, populating the upconversion sample to steady state, can also be used as a CW excitation source when measuring the upconversion quantum yield in a steady-state experiment. An accurately determined value of f enables a more in-depth analysis of the spin statistics of TTA, a factor that so far is not well understood but is critical for the design of new more efficient annihilators [20].

To show the versatility of our new method for determining k_{TTA}, k_T, and I_{th}, it is here illustrated with an example using the very well-known upconversion system with PtOEP as sensitizer and DPA as annihilator (5 µM PtOEP + 1 mM DPA in degassed toluene). The inset in Fig. 7a shows the upconversion emission decay traces

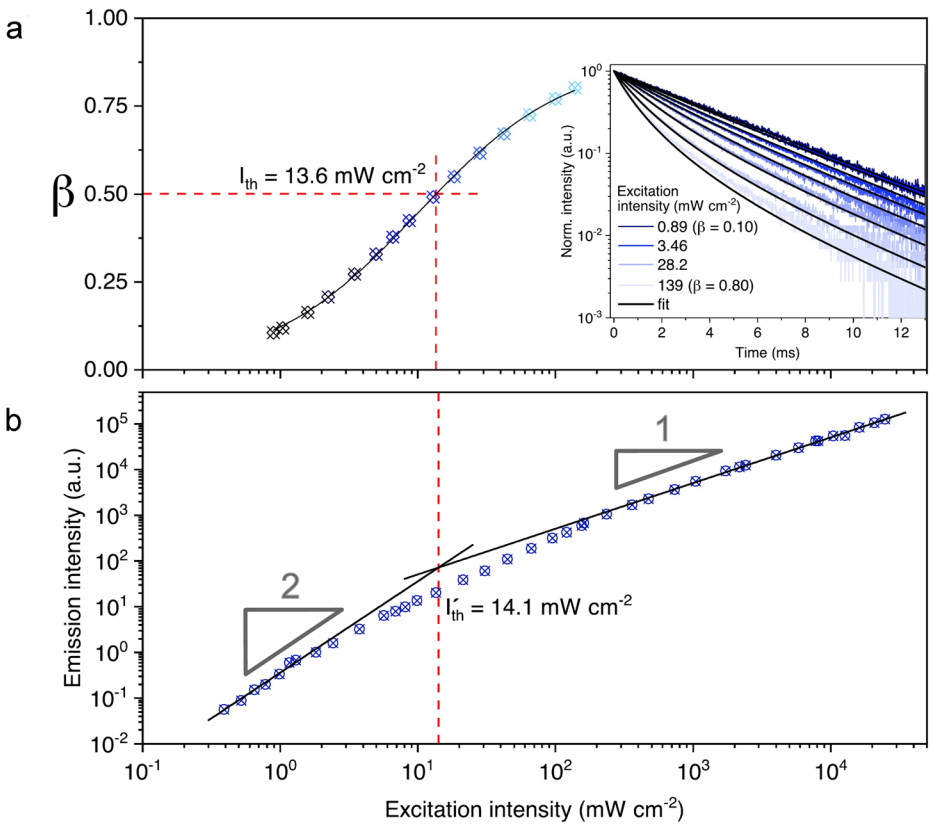

Fig. 7 Threshold intensity for PtOEP (5 µM) + DPA (1 mM) in deaerated toluene determined using **a** the new proposed method, in comparison to **b** using the traditional method. Note that the definition of I_{th} in (**a**) differs from the definition of I'_{th} in (**b**), as described in the text. Inset in **a** shows a selection of the upconversion emission decay traces with the global fit from which β was obtained (the upconversion emission decay traces are the same as shown in Fig. 4a, but here fitted with both k_T and k_{TTA} as global parameters). Black connecting line in a) is a guide to the eye. Black lines in **b** show fit of slope 2 and slope 1 for the low and high excitation intensity regions, respectively

(same data as in Fig. 4a) and how the decay of the upconversion emission signal depends on excitation intensity. The excitation laser was in this experiment modulated with a frequency of 15 Hz, the laser-on time was set to 35 ms to ensure that the sample was populated to steady state, and the emission decay was recorded during the remaining ~ 32 ms of the modulation cycle. From the fit with both k_T and k_{TTA} as global parameters, the rate constants of annihilator triplet decay and TTA were obtained as k_T = 124 s^{-1} and $k_{TTA} = 7.2 \times 10^8$ s^{-1} M^{-1}, which are similar to what previously has been reported [32, 35, 36]. The obtained triplet lifetime ($\tau_T = 1/k_T$) of 8.1 ms is very similar to what was extracted in Fig. 4a, where the same emission decay data were used but fitted with only k_T as global parameter. In the global fit in Fig. 7a, Φ_{isc} and Φ_{TET} were set to unity. For this upconversion sample, these are reasonable assumptions considering that the heavy platinum atom in the sensitizer yields strong spin–orbit coupling and virtually quantitative ISC [54], and the high annihilator concentration and a relatively long sensitizer triplet lifetime (~ 95 µs) results in virtually quantitative TET. It should once again be highlighted that the exact value of k_T depends on the oxygen concentration in the sample, so values reported in the literature can vary depending on how well the sample was degassed. Further, the definition of k_{TTA} varies in the literature and the factor of 2, written explicitly in Eq. 5, is sometimes included in the value of k_{TTA}, so care must be taken when comparing values from different studies. It should also be noted that the extracted values of k_T and k_{TTA} may depend on the relative weight that is put on each decay in the global fit. To yield a uniform weighting, the decay traces can be normalized prior to fitting. However, care should then also be taken during the measurements to ensure that all decay traces have reasonably uniform signal-to-noise ratio, in order to avoid unintentionally putting too much weight on the noisier decay traces in the global fit. For the data shown in Fig. 7a, a constant signal-to-noise ratio was achieved by adjusting the number of averages on the oscilloscope used to record each decay trace so that the PMT signal intensity (in volt) multiplied with the number of averages was kept constant throughout the measurement series.

The threshold intensity for the upconversion sample was determined to I_{th} = 13.6 mW/cm^2, as obtained from the fitted values of β in Fig. 7a. As seen in Fig. 7a, β follows approximately a sigmoidal curve when plotted against the excitation intensity with logarithmic scale on the abscissa. β approaches asymptotically zero and unity at low and high excitation intensities, respectively, which corresponds to the convergence towards slope 2 and slope 1 in the double

logarithmic plot of steady-state upconversion emission intensity versus excitation intensity (Fig. 7b) [55]. Using the traditional method to find the threshold intensity, i.e., graphically identifying the intersect of the two fitted lines of slope 2 and 1 in the plot of upconversion emission intensity versus excitation intensity, the threshold intensity was determined to 14.1 mW/cm^2. A note should be made that the traditional method to determine the threshold intensity has been questioned and reassessed in a recent publication theoretically investigating the excitation intensity dependence of upconversion emission, as discussed in Sect. 5 [44]. It is in this article stated that I_{th}, which formally is defined as the excitation intensity at which the upconversion quantum yield is half of its maximum quantum yield, corresponds to twice the excitation intensity where the fitted lines of slope 2 and slope 1 intersect. By that, the $I_{th} = 13.6$ mW/cm^2 achieved with our new method (Fig. 7a) should be compared to $2 \times 14.1 = 28.2$ mW/cm^2, as achieved with the traditional method (Fig. 7b). The difference between these two values mainly reflects the arbitrariness and subjectiveness of the traditional method that is based on a manual fitting of two lines.

There are many benefits from using our new method for characterizing an upconversion system. The most obvious benefit is the simplicity of the method: With only one experiment that easily can be performed spending less than one day in the lab, all the parameters of k_{TTA}, k_T, Φ_{TTA}, and I_{th} can be obtained from time-resolved emission data. The benefit of using only time-resolved emission data is that emission kinetics is independent on inner filter effects, which otherwise may complicate the analysis when other methods based on quantification of emission intensity from samples with high optical density are used [56]. Further, for determining k_{TTA}, our new method only requires that the absorbance of the sample and the intensity of the excitation source can be measured, parameters that typically are easy to access with high accuracy in comparison to the molar absorptivity of an excited state that is required if k_{TTA} is determined from transient absorption data. For determining I_{th}, our new method has the great benefit that it can be found by only scanning the upconversion emission kinetics within a narrow range of excitation intensities. This is in contrast to the traditional method where the excitation intensity typically must be varied over four or five orders of magnitude to clearly identify the regions where the upconversion emission intensity is assumed to depend quadratically and linearly on excitation intensity. By that, identification of I_{th} directly from the excitation intensity where $\beta = 0.5$ does not require the assumption that the upconversion emission intensity shows a truly quadratic and linear dependence in the low and high excitation intensity regime, assumptions that are not always valid, as discussed in Sect. 5.

Measuring time-resolved upconversion emission can be challenging at low excitation intensities where the emission signal and β is low. Therefore, when using our new method it could be tempting to only measure the emission decay traces at higher excitation intensities where β is higher. In theory, it could work to extract k_{TTA} from such fitted decay traces and identify I_{th} by extrapolation down to $\beta = 0.5$. However, it should be emphasized that the fit is most accurate for the decay traces with β value close 0.5, i.e., far away from the extreme points of $\beta = 0$ and $\beta = 1$. Therefore, it is important that the upconversion emission decay traces that are used in the global fit to determine k_{TTA} and I_{th} are measured under excitation intensities close to and around I_{th}.

As for all methods where experimental data are used to extract a physical parameter, our new method for determining k_{TTA}, k_T, and I_{th} from time-resolved upconversion measurements is based on a couple of assumptions and simplifications. It is important to be aware of these assumptions to understand when the method is applicable and when it is not. First, for Eq. 4 to describe the upconversion emission kinetics, the upconversion sample must consist of a homogeneous material. Otherwise, a more complex expression must be derived, for example by modeling the upconversion emission as originating from a distribution of non-homogeneous upconversion sites [50]. Further, when using Eq. 4 to fit the upconversion emission decay traces it is assumed that the rate of triplet sensitization of the annihilator is fast compared to the time scale of TTA. Only then can the generation of triplet excited annihilators by TET from the sensitizer, which is described by the complicated set of rate equations presented in the Supporting Information, be replaced by the simple factor k_{gen} in Eq. 5. In other words, the TET event should be fast enough so that the triplet excited annihilator can be regarded as being generated directly from the photoexcitation. In practice, this means that the upconversion emission intensity starts decaying immediately when the laser is turned off without delay caused by the sensitizer triplets continuing to generate annihilator triplets. In a typical upconversion system, the annihilator concentration is two or three orders of magnitude higher than the sensitizer concentration, enabling fast TET. If this assumption is not fulfilled, the upconversion emission decay traces must be fitted to the full set of rate equations describing all the relevant species in the system. The second assumption is that the volume element in the sample that is photoexcited and viewed by the detector is homogeneously excited. This is an important, but rarely considered, assumption that applies to all types of upconversion experiments where a parameter is to be quantified in relation to the excitation intensity, e.g., upconversion emission intensity, quantum yield, or upconversion kinetics. The intensity of the excitation light attenuates when it travels through a sample, as described by Lambert–Beer´s law. Therefore, the concentration of excited chromophores, and thereby also the rate of bimolecular TTA, varies within the sample. Because of this, it is not trivial to relate, for

example, the upconversion emission intensity to a certain excitation intensity if the optical density is too high. To ensure a homogeneous excitation volume, we recommend adjusting the thickness or concentration of the sample to keep its optical density at the excitation wavelength well below 0.1, which means that the attenuation of excitation light through the sample is below ~ 20%. In addition to these assumptions, it should be noted that, to determine k_{TTA} with this new method, it must be possible to accurately measure the absorbance of the sample. This is typically not a problem for upconversion systems of dissolved chromophores in solution, but it can be an issue for non-transparent upconversion samples that scatters light. However, we want to highlight that k_T,β, and I_{th} can be determined with the new method even without knowing the absorbance of the sample.

7 Conclusion

In this perspective, several parameters important in TTA-UC experiments have been discussed and analyzed. Triplet state energies may be extracted from phosphorescence measurements, and we highlight that this can be achieved by excitation into either the singlet or the triplet manifold, using ZnOEP as a model compound. The triplet energy may also be extracted from bimolecular quenching experiments, and we argue that this methodology might be more accurate and relevant in some situations. Triplet lifetimes (τ_T) are preferably measured using time-resolved emission of either phosphorescence/delayed fluorescence (for sensitizers) or of upconverted light (for annihilators). A comparison between different strategies to extract τ_T is undertaken. Using PtOEP/DPA as a model system, we show that the most accurate values are obtained by investigating the excitation intensity dependence of the observed kinetics and then employ a global fitting procedure. Using a square-pulse excitation and by modifying the global fitting procedure used to determine τ_T, the same measurements can also be used to extract the somewhat elusive rate constant for TTA—which previously has relied on challenging nanosecond transient absorption measurements—as well as to determine the excitation threshold intensity (I_{th}). All of this is achieved using a versatile experimental setup where the only crucial components are excitation sources in the form of commercially available CW laser diodes that can be modulated, and an emission detector. We show that the new method yields similar I_{th} to the method based on steady-state measurements that is commonly used. The new method also benefits from that a smaller range of excitation intensities can be used while still obtaining an accurate value. This method also serves to accurately estimate the TTA quantum yield, a parameter that is important for further analysis of, e.g., the spin-statistical factor. The collection of methods presented herein provide an experimental framework that will hopefully aid the TTA-UC community in the strive for efficient, facile, and accurate determination of the important parameters discussed herein.

Supplementary Information The online version contains supplementary material available at https://doi.org/10.1007/s43630-022-00219-x.

Funding Open access funding provided by Chalmers University of Technology. We are grateful to The Swedish Energy Agency (contract 46526-1) and the Swedish Research Council for providing financial support.

Declarations

Conflict of interest On behalf of all the authors, the corresponding author states that there is no conflict of interest.

References

1. Parker, C. A., & Hatchard, C. G. (1962). Delayed fluorescence from solutions of anthracene and phenanthrene. *Proceeding of Royal Society of London Series A Mathematics Physics Science, 269*(1339), 574–584. https://doi.org/10.1098/rspa.1962.0197
2. Trupke, T., Green, M. A., & Würfel, P. (2002). Improving solar cell efficiencies by up-conversion of sub-band-gap light. *Journal of Applied Physics, 92*(7), 4117–4122. https://doi.org/10.1063/1.1505677
3. Islangulov, R. R., Lott, J., Weder, C., & Castellano, F. N. (2007). Noncoherent low-power upconversion in solid polymer films. *Journal of the American Chemical Society, 129*(42), 12652–12653. https://doi.org/10.1021/ja075014k
4. Gray, V., Moth-Poulsen, K., Albinsson, B., & Abrahamsson, M. (2018). Towards efficient solid-state triplet–triplet annihilation based photon upconversion: Supramolecular, macromolecular and self-assembled systems. *Coordination Chemistry Reviews, 362*, 54–71. https://doi.org/10.1016/j.ccr.2018.02.011
5. Ahmad, W., Wang, J., Li, H., Ouyang, Q., Wu, W., & Chen, Q. (2021). Strategies for combining triplet–triplet annihilation upconversion sensitizers and acceptors in a host matrix. *Coordination Chemistry Reviews, 439*, 213944. https://doi.org/10.1016/j.ccr.2021.213944
6. Sasaki, Y., Amemori, S., Yanai, N., & Kimizuka, N. (2021). Singlet-to-triplet absorption for near-infrared-to-visible photon upconversion. *Bulletin Chemical Society of Japan, 94*(6), 1760–1768. https://doi.org/10.1246/bcsj.20210114

7. Gray, V., Allardice, J. R., Zhang, Z., & Rao, A. (2021). Organic-quantum dot hybrid interfaces and their role in photon fission/fusion applications. *Chemistry Physics Reviews, 2*(3), 31305. https://doi.org/10.1063/5.0050464
8. Beery, D., Schmidt, T. W., & Hanson, K. (2021). Harnessing sunlight via molecular photon upconversion. *ACS Applied Materials and Interfaces, 13*(28), 32601–32605. https://doi.org/10.1021/acsami.1c08159
9. Dexter, D. L. (1953). A theory of sensitized luminescence in solids. *The Journal of Chemical Physics, 21*(5), 836–850. https://doi.org/10.1063/1.1699044
10. Zhou, Y., Castellano, F. N., Schmidt, T. W., & Hanson, K. (2020). On the quantum yield of photon upconversion via triplet-triplet annihilation. *ACS Energy Letters, 5*(7), 2322–2326. https://doi.org/10.1021/acsenergylett.0c01150
11. Gray, V., Dzebo, D., Abrahamsson, M., Albinsson, B., & Moth-Poulsen, K. (2014). Triplet-triplet annihilation photon-upconversion: Towards solar energy applications. *Physical Chemistry Chemical Physics: PCCP, 16*(22), 10345–10352. https://doi.org/10.1039/C4CP00744A
12. Isokuortti, J., Allu, S. R., Efimov, A., Vuorimaa-Laukkanen, E., Tkachenko, N. V., Vinogradov, S. A., Laaksonen, T., & Durandin, N. A. (2020). Endothermic and exothermic energy transfer made equally efficient for triplet-triplet annihilation upconversion. *Journal of Physical Chemistry Letters, 11*(1), 318–324. https://doi.org/10.1021/acs.jpclett.9b03466
13. Olesund, A., Johnsson, J., Edhborg, F., Ghasemi, S., Moth-Poulsen, K., & Albinsson, B. (2022). Approaching the spin-statistical limit in visible-to-ultraviolet photon upconversion. *Journal of the American Chemical Society, 144*(8), 3706–3716. https://doi.org/10.1021/jacs.1c13222
14. Meroni, D., Monguzzi, A., & Meinardi, F. (2020). Photon upconversion in multicomponent systems: Role of back energy transfer. *The Journal of Chemical Physics, 153*(11), 114302. https://doi.org/10.1063/5.0021253
15. Edhborg, F., Bildirir, H., Bharmoria, P., Moth-Poulsen, K., & Albinsson, B. (2021). Intramolecular triplet-triplet annihilation photon upconversion in diffusionally restricted anthracene polymer. *The Journal of Physical Chemistry B, 125*(23), 6255–6263. https://doi.org/10.1021/acs.jpcb.1c02856
16. Wu, T. C., Congreve, D. N., & Baldo, M. A. (2015). Solid state photon upconversion utilizing thermally activated delayed fluorescence molecules as triplet sensitizer. *Applied Physics Letters, 107*(3), 31103. https://doi.org/10.1063/1.4926914
17. Yanai, N., Kozue, M., Amemori, S., Kabe, R., Adachi, C., & Kimizuka, N. (2016). Increased vis-to-UV upconversion performance by energy level matching between a TADF donor and high triplet energy acceptors. *Journal of Material Chemistry C, 4*(27), 6447–6451. https://doi.org/10.1039/C6TC01816E
18. Zähringer, T. J. B., Bertrams, M.-S., & Kerzig, C. (2022). Purely organic Vis-to-UV upconversion with an excited annihilator singlet beyond 4 eV. *Journal of Material Chemistry C*. https://doi.org/10.1039/D1TC04782E
19. Wang, X., Tom, R., Liu, X., Congreve, D. N., & Marom, N. (2020). An energetics perspective on why there are so few triplet–triplet annihilation emitters. *Journal of Material Chemistry C, 8*(31), 10816–10824. https://doi.org/10.1039/D0TC00044B
20. Bossanyi, D. G., Sasaki, Y., Wang, S., Chekulaev, D., Kimizuka, N., Yanai, N., & Clark, J. (2021). Spin statistics for triplet-triplet annihilation upconversion: Exchange coupling, intermolecular orientation, and reverse intersystem crossing. *JACS Au, 1*(12), 2188–2201. https://doi.org/10.1021/jacsau.1c00322
21. Zhang, Q., Komino, T., Huang, S., Matsunami, S., Goushi, K., & Adachi, C. (2012). Triplet exciton confinement in green organic light-emitting diodes containing luminescent charge-transfer Cu(I) complexes. *Advances Function Materials, 22*(11), 2327–2336. https://doi.org/10.1002/adfm.201101907
22. Marchetti, A. P., & Kearns, D. R. (1967). Investigation of singlet-triplet transitions by the phosphorescence excitation method. IV. the singlet-triplet absorption spectra of aromatic hydrocarbons. *Journal of America Chemistry Society, 89*(4), 768–777. https://doi.org/10.1021/ja00980a007
23. Kasha, M. (1952). Collisional perturbation of spin-orbital coupling and the mechanism of fluorescence quenching. A visual demonstration of the perturbation. *Journal of Chemistry Physics, 20*(1), 71–74. https://doi.org/10.1063/1.1700199
24. Giachino, G. G., & Kearns, D. R. (1970). Nature of the external heavy-atom effect on radiative and nonradiative singlet-triplet transitions. *The Journal of Chemical Physics, 52*(6), 2964–2974. https://doi.org/10.1063/1.1673425
25. Merkel, P. B., & Dinnocenzo, J. P. (2008). Thermodynamic energies of donor and acceptor triplet states. *Journal of Photochemistry Photobiology A Chemistry, 193*(2), 110–121. https://doi.org/10.1016/j.jphotochem.2007.06.014
26. Sandros, K. (1964). Transfer of triplet state energy in fluid systems III. Reversible energy transfer. *Acta Chemica Scandinavica, 18*(10), 2355–2374. https://doi.org/10.3891/acta.chem.scand.18-2355
27. Sandros, K., & Bäckström, H. L. J. (1962). Transfer of triplet state energy in fluid solutions. *Acta Chemica Scandinavica, 16*(4), 958–968. https://doi.org/10.3891/acta.chem.scand.16-0958
28. Balzani, V., & Bolletta, F. (1978). Energy transfer processes involving distorted excited states. *Journal of the American Chemical Society, 100*(23), 7404–7405. https://doi.org/10.1021/ja00491a044
29. de Carvalho, I. M. M., & Gehlen, M. H. (1999). The solvent effect on electronic energy transfer between excited [Ru(bpy)3]2+ donor and aromatic acceptors. *Journal of Photochemistry Photobiology A Chemistry, 122*(2), 109–113. https://doi.org/10.1016/S1010-6030(99)00014-3
30. Harada, N., Sasaki, Y., Hosoyamada, M., Kimizuka, N., & Yanai, N. (2021). Discovery of key TIPS-naphthalene for efficient visible-to-UV photon upconversion under sunlight and room light. *Angewandte Chemie, 133*(1), 144–149. https://doi.org/10.1002/anie.202012419
31. Yin, W., Yu, T., Chen, J., Hu, R., Yang, G., Zeng, Y., & Li, Y. (2021). Thermally activated upconversion with metal-free sensitizers enabling exceptional anti-stokes shift and anti-counterfeiting application. *ACS Applied Materials and Interfaces, 13*(48), 57481–57488. https://doi.org/10.1021/acsami.1c19181
32. Olesund, A., Gray, V., Mårtensson, J., & Albinsson, B. (2021). Diphenylanthracene dimers for triplet-triplet annihilation photon upconversion: Mechanistic insights for intramolecular pathways and the importance of molecular geometry. *Journal of the American Chemical Society, 143*(15), 5745–5754. https://doi.org/10.1021/jacs.1c00331
33. Saenz, F., Ronchi, A., Mauri, M., Vadrucci, R., Meinardi, F., Monguzzi, A., & Weder, C. (2021). Nanostructured polymers enable stable and efficient low-power photon upconversion. *Advanced Functional Materials, 31*(1), 2004495. https://doi.org/10.1002/adfm.202004495
34. Gao, C., Prasad, S. K. K., Zhang, B., Dvořák, M., Tayebjee, M. J. Y., McCamey, D. R., Schmidt, T. W., Smith, T. A., & Wong, W. W. H. (2019). Intramolecular versus intermolecular triplet fusion in multichromophoric photochemical upconversion. *Journal of Physical Chemistry C, 123*(33), 20181–20187. https://doi.org/10.1021/acs.jpcc.9b07098
35. Gray, V., Dreos, A., Erhart, P., Albinsson, B., Moth-Poulsen, K., & Abrahamsson, M. (2017). Loss channels in triplet-triplet annihilation photon upconversion: Importance of annihilator singlet and triplet surface shapes. *Physical Chemistry Chemical Physics:*

PCCP, 19(17), 10931–10939. https://doi.org/10.1039/C7CP01368J
36. Gray, V., Dzebo, D., Lundin, A., Alborzpour, J., Abrahamsson, M., Albinsson, B., & Moth-Poulsen, K. (2015). Photophysical characterization of the 9,10-disubstituted anthracene chromophore and its applications in triplet–triplet annihilation photon upconversion. *Journal of Material Chemistry C, 3*(42), 11111–11121. https://doi.org/10.1039/C5TC02626A
37. Ronchi, A., Capitani, C., Pinchetti, V., Gariano, G., Zaffalon, M. L., Meinardi, F., Brovelli, S., & Monguzzi, A. (2020). High photon upconversion efficiency with hybrid triplet sensitizers by ultrafast hole-routing in electronic-doped nanocrystals. *Advanced Materials, 32*(37), 2002953. https://doi.org/10.1002/adma.202002953
38. Hou, L., Olesund, A., Thurakkal, S., Zhang, X., & Albinsson, B. (2021). Efficient visible-to-UV photon upconversion systems based on CdS nanocrystals modified with triplet energy mediators. *Advanced Functional Material, 31*(47), 2106198. https://doi.org/10.1002/adfm.202106198
39. He, S., Han, Y., Guo, J., & Wu, K. (2021). Long-lived delayed emission from CsPbBr 3 perovskite nanocrystals for enhanced photochemical reactivity. *ACS Energy Letters, 6*(8), 2786–2791. https://doi.org/10.1021/acsenergylett.1c01291
40. Singh-Rachford, T. N., & Castellano, F. N. (2009). Low power visible-to-UV upconversion. *Journal of Physical Chemistry A, 113*(20), 5912–5917. https://doi.org/10.1021/jp9021163
41. Ye, C., Gray, V., Mårtensson, J., & Börjesson, K. (2019). Annihilation versus excimer formation by the triplet pair in triplet-triplet annihilation photon upconversion. *Journal of the American Chemical Society, 141*(24), 9578–9584. https://doi.org/10.1021/jacs.9b02302
42. Glaser, F., Kerzig, C., & Wenger, O. S. (2021). Sensitization-initiated electron transfer via upconversion: Mechanism and photocatalytic applications. *Chemical Science, 12*(29), 9922–9933. https://doi.org/10.1039/D1SC02085D
43. Schmid, L., Glaser, F., Schaer, R., & Wenger, O. S. (2022). High triplet energy iridium(III) isocyanoborato complex for photochemical upconversion, photoredox and energy transfer catalysis. *Journal of the American Chemical Society, 144*(2), 963–976. https://doi.org/10.1021/jacs.1c11667
44. Murakami, Y., & Kamada, K. (2021). Kinetics of photon upconversion by triplet–triplet annihilation: A comprehensive tutorial. *Physical Chemistry Chemical Physics: PCCP, 23*(34), 18268–18282. https://doi.org/10.1039/D1CP02654B
45. Monguzzi, A., Mezyk, J., Scotognella, F., Tubino, R., & Meinardi, F. (2008). Upconversion-induced fluorescence in multicomponent systems: Steady-state excitation power threshold. *Physical Review B, 78*(19), 195112. https://doi.org/10.1103/PhysRevB.78.195112
46. Haefele, A., Blumhoff, J., Khnayzer, R. S., & Castellano, F. N. (2012). Getting to the (square) root of the problem: How to make noncoherent pumped upconversion linear. *Journal of Physical Chemistry Letters, 3*(3), 299–303. https://doi.org/10.1021/jz300012u
47. Cheng, Y. Y., Khoury, T., Clady, R. G. C. R., Tayebjee, M. J. Y., Ekins-Daukes, N. J., Crossley, M. J., & Schmidt, T. W. (2010). On the efficiency limit of triplet–triplet annihilation for photochemical upconversion. *Physical Chemistry Chemical Physics: PCCP, 12*(1), 66–71. https://doi.org/10.1039/B913243K
48. Dzebo, D., Börjesson, K., Gray, V., Moth-Poulsen, K., & Albinsson, B. (2016). Intramolecular triplet-triplet annihilation upconversion in 9,10-diphenylanthracene oligomers and dendrimers. *Journal of Physical Chemistry C, 120*(41), 23397–23406. https://doi.org/10.1021/acs.jpcc.6b07920
49. Lissau, J. S., Nauroozi, D., Santoni, M.-P., Edvinsson, T., Ott, S., Gardner, J. M., & Morandeira, A. (2015). What limits photon upconversion on mesoporous thin films sensitized by solution-phase absorbers? *Journal of Physical Chemistry C, 119*(9), 4550–4564. https://doi.org/10.1021/jp5118129
50. Ronchi, A., & Monguzzi, A. (2021). Developing solid-state photon upconverters based on sensitized triplet–triplet annihilation. *Journal of Applied Physics, 129*(5), 050901. https://doi.org/10.1063/5.0034943
51. Bachilo, S. M., & Weisman, R. B. (2000). Determination of triplet quantum yields from triplet−triplet annihilation fluorescence. *Journal of Physical Chemistry A, 104*(33), 7711–7714. https://doi.org/10.1021/jp001877n
52. Cheng, Y. Y., Fückel, B., Khoury, T., Clady, R. G. C. R., Tayebjee, M. J. Y., Ekins-Daukes, N. J., Crossley, M. J., & Schmidt, T. W. (2010). Kinetic analysis of photochemical upconversion by triplet−triplet annihilation: Beyond any spin statistical limit. *Journal of Physical Chemistry Letters, 1*(12), 1795–1799. https://doi.org/10.1021/jz100566u
53. Sun, W., Ronchi, A., Zhao, T., Han, J., Monguzzi, A., & Duan, P. (2021). Highly efficient photon upconversion based on triplet–triplet annihilation from bichromophoric annihilators. *Journal of Material Chemistry C, 9*(40), 14201–14208. https://doi.org/10.1039/D1TC01569A
54. Ponterini, G., Serpone, N., Bergkamp, M. A., & Netzel, T. L. (1983). Comparison of radiationless decay processes in osmium and platinum porphyrins. *Journal of the American Chemical Society, 105*(14), 4639–4645. https://doi.org/10.1021/ja00352a020
55. Auckett, J. E., Chen, Y. Y., Khoury, T., Clady, R. G. C. R., Ekins-Daukes, N. J., Crossley, M. J., & Schmidt, T. W. (2009). Efficient up-conversion by triplet-triplet annihilation. *Journal of Physics: Conference Series, 185*, 12002. https://doi.org/10.1088/1742-6596/185/1/012002
56. Kubista, M., Sjoback, R., Eriksson, S., & Albinsson, B. (1994). Experimental correction for the inner-filter effect in fluorescence spectra. *The Analyst, 119*(3), 417–419. https://doi.org/10.1039/AN9941900417